BJRS

BRAZILIAN JOURNAL
OF
RADIATION SCIENCES
09-01A (2021) 01-17

Characterization of the petrology of the tar sandstone rock of the Paraná basin

Amadeu[a] R. A., Bernardes[a] T. L. S., Santos[a] R. S., Garcia[a] R. H. L., Velo[a] A. F., Cavallaro[b] F. A., Mesquita C. H., Hamada[a] M. M

[a] *Instituto de Pesquisas Energéticas e Nucleares (IPEN/CNEN-SP), 05508-000, São Paulo-SP, Brazil*
thiagolsbernardes@gmail.com

[b] *Universidade Cidade de São Paulo (UNICID), 03071-000, São Paulo-SP, Brazil*
assiscavallaro@gmail.com

ABSTRACT

In the state of São Paulo (Brazil), occurrences of tar sandstone are known in Botucatu, Angatuba, Pirambóia, Anhembi and Bofete municipalities. In the present work a sample of white tar sandstone was taken from Anhembi municipality, located at Km 168 of the Castelo Branco Highway. In the petroleum area, sandstones act as excellent hydrocarbon reservoirs, since they have specific characteristics, such as: high porosity and permeability. Porosity is a property of rocks, and it may be understood as the voids contained in the matrix (where fluids remain stored), while permeability is the ability of the rock to transmit these stored fluids. Due to these characteristics of sandstones, researchers have shown a growing interest in the study and characterization of this type of rock, which is a fundamental element of an oil system. In the present work, four characterization techniques were used in the Anhembi tar sandstone sample, namely: X-ray Diffraction (XRD), X-ray Fluorescence (XRF), Scanning Electron Microscope (SEM) and the third generation Industrial Computerized Tomography. Through these techniques, the chemical composition, grain morphology, crystalline structure phases and an image of a slice of the internal structure of the white tar sandstone sample were obtained.

Keywords: **Tar sandstone, Characterization, Gamma ray computed industrial tomography.**

ISSN: 2319-0612
Accepted: 2020-11-19

1. INTRODUCTION

Sandstones may be defined as sedimentary rocks composed of fragments of sand minerals. Sandstones are mixtures of mineral grains and fragments from the erosion of various types of rocks. The grains that form the sandstones are generally from mineral quartz, but, they may be from any other mineral (mainly the feldspar) or the lithic fragment (from a rock), since they have the dimensions of the sand grains from tar sandstones (or bituminous sandstones) [1].

In the petroleum area, the sandstones act as excellent reservoirs of hydrocarbons, since they have specific characteristics, such as: high porosity and permeability. Porosity is a property of rocks, and it may be understood as the empty spaces contained in their matrix (where fluids remain stored), while permeability is the rock ability to transmit these stored fluids. There are a large number of studies carried out in the Paraná Basin related to geological factors, such as stratigraphy, structural framework, temporal aspects and others, helping the understanding of hydrocarbons generation and migration processes [2].

The outcrops of tar sandstones (or bituminous sandstones) from Pirambóia Formation, in the State of São Paulo, Brazil, constitute one of the most important oil occurrences in Paraná Basin, since the volume of these outcrops vastly outstrips the volume of small accumulations discovered in the subsurface [3,4]. There are, approximately, 25 occurrences of tar sandstones in Anhembi, Bofete, Guareí and Angatuba cities. This formation consists of white, gray, yellowish and reddish sandstones, with medium and large cross-stratifications plus plane-parallel laminations. The tar sandstones are composed of siliciclastic grains impregnated in the pores by heavy asphalt-like oil. On average, asphaltic sandstones contain 10-15% oil, the remainder being composed of the mineral matrix [5,4]. The sandstone samples were collected in Anhembi city, São Paulo state, and they are represented in the map of Figure 1.

Figure 1: *Region of the Paraná Basin in the state of São Paulo, where the tar sandstones were collected.*

Due to the increasing demand for mineral and energy resources, water and hydrocarbons more specifically, plus the increasing complexity to obtain them, the development of new technologies for the exploration of these sources is required.

Over the years, geophysics and geology have both been used as tools for the petrophysical characterization of oil and gas storage sandstones [6]. More recently, the computerized tomography technique has been used for the structural analysis of the rocks in geoscience, using X-ray microtomography [7-9].

The use of the industrial computed tomography technique may be considered a technological innovation, since it allows the limitations of the geophysical and microtomographical techniques to be overcome, without processing the samples for structural analysis of the rocks in geoscience. As far as we know, no work using industrial tomographers, in the area of geoscience, has been found. The technique of industrial tomography is a non destructive technique that permits measurements of rocks of larger dimensions and different geometries, with their reconstruction in three-dimensional (3D) images. Additionally, the images may be analyzed in slices for visualizing important parts of the rock, improving the understanding of its internal structure.

The knowledge of the physical properties of the rock related to the filling of fluids in its pores, its structural properties and its internal geometry may contribute, significantly, to the exploration and

recovery of hydrocarbons from the asphalt rock reservoirs, providing subsidies to oil engineers in the recovery of hydrocarbons (oil) from their interior, having a significant economic impact.

For the development of the present work, a sample of tar sandstone from the Paraná Basin was studied and characterized, using a third-generation industrial computerized tomograph with gamma radiation, developed at IPEN/CNEN Radiation Technology Center (CTR) -SP [10-12]. Complementary techniques, such as X-ray diffraction (XRD), scanning electron microscopy (SEM) and X-ray fluorescence (XRF) were used to provide additional characterization information.

2. MATERIALS AND METHODS

2.1 Sample collection

Initially, the sample of the tar sandstone from the Paraná Basin was obtained through the use of specific hammers for field work in outcrops. The region selected for the extraction of the sample is located in the region of Anhembi city, SP. After the collection, some characterization techniques were carried out to obtain important information about the morphology, image of the internal structure and chemical composition of the tar sandstone. To obtain the image of the internal structure, the sample was used in full by the computerized industrial tomograph developed at IPEN. For X-ray fluorescence measurement, about 0.009 Kg of tar sandstone was pulverized. For the X-ray diffraction measurement, around 0.002 Kg of sample powder, pulverized from the sample collected, was used. For the scanning electron microscope measurement, less than one gram of the pulverized rock was covered with carbon, which is the material that more easily conducts the incident beam electrons. The sample was pulverized at the Institute of Geosciences of USP (IGC).

2.2 X-Ray Fluorescence (XRF)

X-ray fluorescence spectrometry is a non-destructive technique to identify the elements present in a sample (qualitative analysis), as well as to establish the proportion (concentration) in which each element is present in the sample. In X-ray fluorescence spectrometry, a high energy radiation source (Gamma radiation or X radiation) causes the excitation of the atoms present in the substance to be analyzed. When an atom in the ground state is under the action of an external source of energy (e.g.

: X-rays), it absorbs this energy, promoting electrons to more energetic levels. In this state, the atom will be in an unstable situation, called "Excited State".

X-ray fluorescence spectrometry analysis is based on the fact that the chemical elements emit characteristic radiations when subjected to proper excitation. The emission of characteristic line spectra may be induced by the impact of accelerated particles, such as electrons, protons, alpha particles and ions.

An atom receiving an X-ray discharge allows the entrance of X-ray photons that reach an electron, which is withdrawn from the lower energy atomic layer, leaving a void (Figure 2). This emptiness is filled with a higher energy electron. In the process, there is a release of energy (fluorescence) detached in the form of an X-ray photon.[13]. The X-ray fluorescence used in this work was a Bruker s8 Tiger model.

Figure 2: *X-Ray representation.*

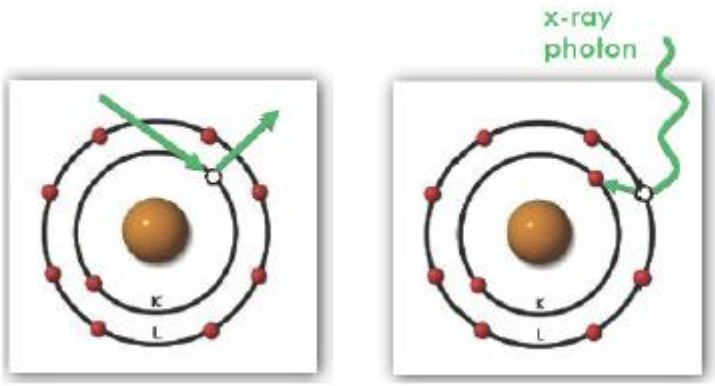

2.3 X-Ray Diffraction (XRD)

X-ray diffraction corresponds to one of the main techniques of microstructural characterization of crystalline materials, with applications in several fields of knowledge, more particularly in materials engineering and science and geoscience, among other areas.

X-rays, when reaching any material, may be elastically mirrored, without loss of energy by the electrons of an atom (dispersion or coherent scattering). The X-ray photon, after the collision with

the electron, changes its trajectory, maintaining, however, the same phase and energy of the incident photon. From the point of view of wave physics, it could be said that the electromagnetic wave is, instantly, absorbed by the electron and re-emitted: each electron acts, therefore, like a center of an X-ray emission.

Considering two or more planes of a crystalline structure, the conditions for X-ray diffraction (constructive interference) will depend on the path difference traveled by X-rays and the wavelength of the incident radiation. This condition is expressed by Bragg's law, i.e. $n\lambda = 2d \sin \theta$ (Figure 3), where λ corresponds to the wavelength of the incident radiation, "n" to an integer (diffraction order), "d" at a distance interplanar for the set of hkl planes (Miller indices) of the crystalline structure, and θ to the angle of incidence of the X-rays (measured between the beam and the crystalline planes) [14]. The diffractometer used in this work is from Bruker d8 Advance model**.**

Figure 3: *X-Ray diffraction.*

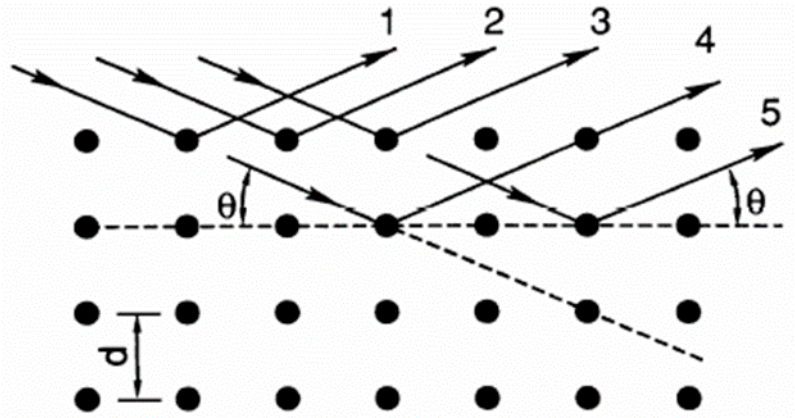

2.4 Scanning Electron Microscopy (SEM)

A scanning electron microscope (SEM) uses a beam of electrons in place of photons employed in a conventional light microscope, solving the problem of resolution related to the white light source. As a result, modern appliances allow increases of 300,000 times or more for most solid materials, while maintaining the depth of field consistent with the observation of rough surfaces. SEM is a

device that may quickly provide information on the morphology and identification of chemical elements in a solid sample. SEM is one of the most versatile instruments available for the observation and analysis of microstructural characteristics of solid objects.

The main reason for its utility is the high resolution that may be obtained when the samples are observed; values in the order of 2 to 5 nanometers are usually presented by commercial instruments, while advanced research instruments are capable of achieving a resolution better than 1 nm.

The principle of a scanning electron microscope (SEM) is the use a small diameter electron beam to scan the surface of the sample, point by point, in successive lines and transmit the detector signal to a cathode screen whose scanning is perfectly synchronized with that of the incident beam. By a system of deflection coils, the beam can be guided so as to sweep the surface of the sample along a rectangular mesh. The image signal results from the interaction of the incident beam with the surface of the sample. The signal collected by the detector is used to modulate the brightness of the monitor, allowing observation. Most instruments use a heated tungsten filament (W) as the source of electrons, operating in a range of 1 to 50 kV acceleration voltages. The beam is accelerated by the high voltage created between the filament and the anode. It is, then, focused on the sample by a series of three electromagnetic lenses with a spot smaller than 4 nm. The beam interacting with the sample produces electrons and photons that can be collected by suitable detectors and converted into a video signal [15].

2.5 Third generation industrial tomograph

The principle of Computed Tomography scanning by transmission consists of the transmission of Gamma rays through a heterogeneous medium accompanied by attenuation, which provides the measure of the integral beam in the mass distribution line through the path traveled by the beam. The measurement of several beams with different orientations, both spatial and angular in relation to the studied volume, followed by an image reconstruction process, provides the density distribution of the phases with a high degree of spatial resolution [16]. A computational system is used to reconstruct the tomographic image of a cross section studied (observed by the detectors).

The third generation industrial tomograph developed in the CTR consists of an arrangement with fifteen 12.5 mm diameter x 50 mm thick NaI (Tl) detectors, positioned diametrically opposite to an

Ir-192 radioactive source. The associated electronics and data acquisition system coupled to the tomograph were developed in the CTR / IPEN, as shown in Figure 4.

Figure 4: *Third - generation industrial tomograph developed at IPEN / CNEN–SP.*

3. RESULTS AND DISCUSSION

The chemical composition of tar sandstone, measured by the X-ray fluorescence method, is summarized in table 1. As it may be observed in this table, the elements with the highest concentration in the sample were: Si (23.9%), Al (7.44%) and K (1.44%). Other elements in a lower concentration were, also, found (in the order of PPM). Some elements found in very low concentrations were Rb (47.2 ppm), S (43 ppm), Zn (24 ppm), Cu (20.9 ppm), Pb (14.9 ppm), among others.

Table 1: Chemical composition of the tar sandstone from Anhembi - SP.

Formula	Z	Concentration	Error
Si	14	23.9%	0.129%
Al	13	7.44%	0.241%
K	19	1.44%	0.410%
Mg	12	1.31%	0.567%
Fe	26	1.00%	0.186%
Ca	20	0.285%	0.897%
Na	11	0.251%	2.62%
Ti	22	0.197%	0.935%
Ba	56	454 ppm	4.44%
P	15	406 ppm	3.29%
Zr	40	201 ppm	0.491%
Mn	25	183ppm	2.16%
Sr	38	73.4ppm	1.20%

Another technique used for tar sandstone characterization was the X-ray diffraction. This technique allows the phase peaks of the crystalline structures to be present in the sample. The first step was the construction of the diffractogram, based on the measurements obtained by the X-ray diffractometer. This diffractogram was generated with the aid of Software Origin. Then, another software (EVA) was used to identify the crystalline phase peaks of the, previously, generated diffractogram. For this identification, a ready database called PDF 2003, within the EVA Software, was used. Such database is represented by Figures 5 and 6.

Figure 5: *Ray X diffractogram of tar sandstone from Paraná Basin and EVA software database for identifying the crystalline phase peak, with abscissa range from 13 to 30 Two Theta.*

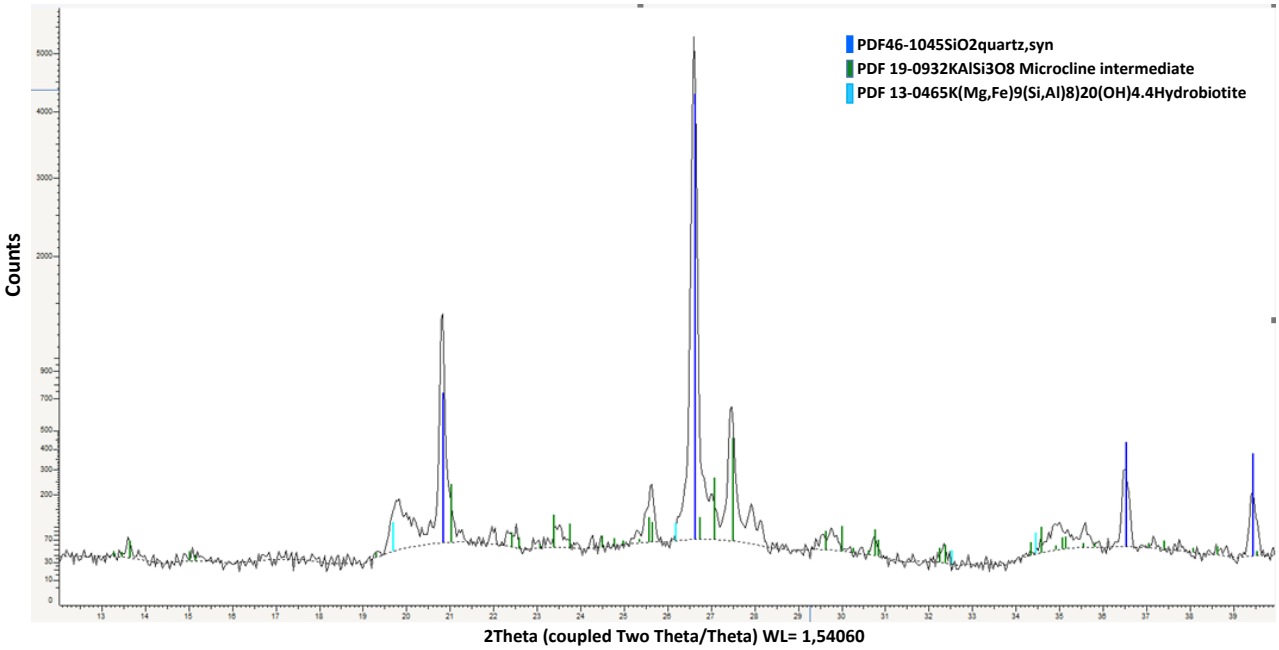

Figure 6: *Continuation of figure 5, with abscissa range from 13 to 30 Two Theta.*

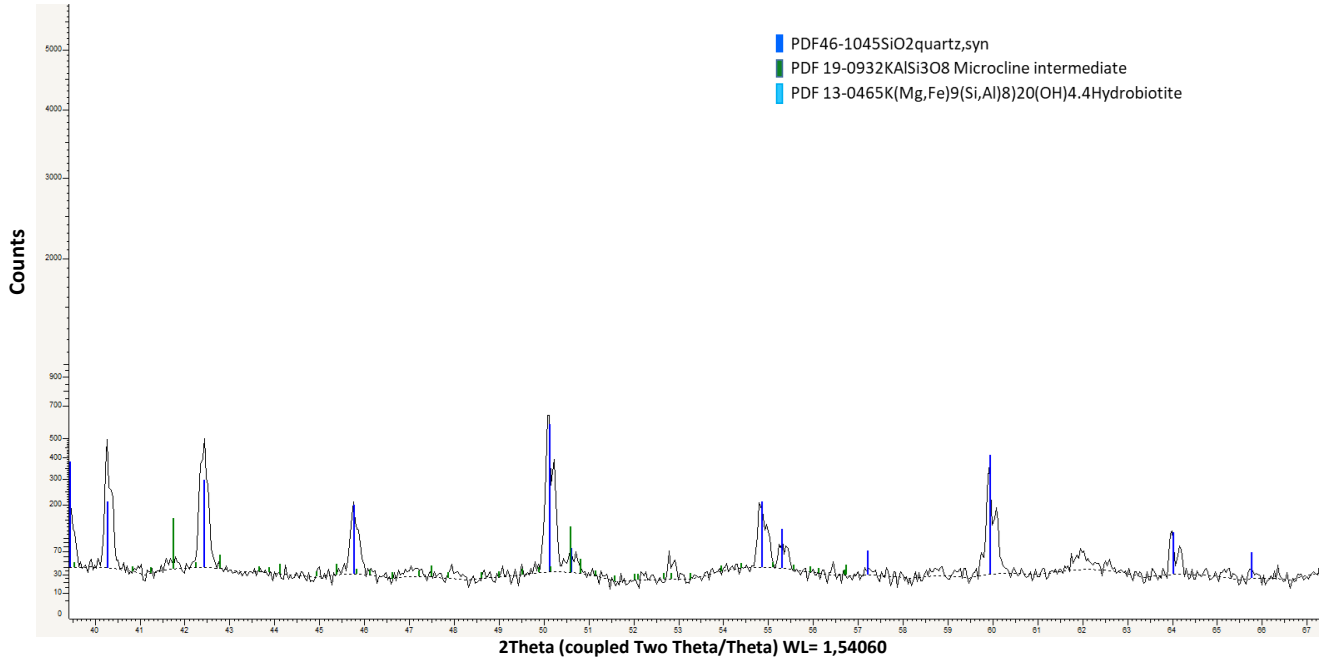

Figure 7 illustrates the diffractogram generated in the Origin Software, with the crystalline phase peaks highlighted by circles. Identification was based on EVA PDF 2003 database, presented in Figures 5 and 6. According to the database, the crystalline phase that was identified in higher intensity (larger peaks) was Quartz (SiO_2). Other crystalline phases at lower intensities were, also, identified, namely: Microcline ($KALSi_3O_8$) and Hydrobiotite $K(Mg,Fe^{2+})_6((Si,Al)_8O_{20})(OH)_4 \cdot nH_2O$). At angles from 70 degrees onwards, virtually no crystalline phase peaks were identified.

Figure 7: *Diffractogram generated by Software Origin with the peaks of the main crystalline phases.*

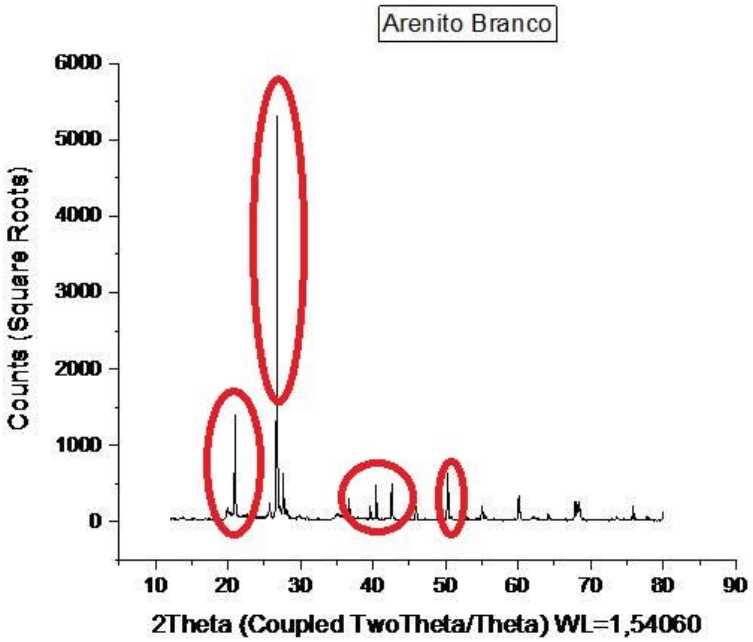

Figures 8, 9 and 10 represent the images of tar sandstone obtained by the scanning electron microscope. Different amplitudes were used during the application of the method to obtain more detailed sample information. Figure 8 illustrates some empty spaces of the sample that may contain the oil in question (highlighted in red circle), representing the porosity, typical of a reservoir rock (oil in the case of the present work). Figure 9 used 1500-fold amplitude, which allows the observation of the morphology of the grains particles that make up the asphalt sandstone. Through this figure, it was possible to observe that there is no cementation between the grains, indicating that the sandstone analyzed in the present work has the characteristic of a good hydrocarbon reservoir, since the cementation between the grains can impair the permeability (connection between the grains), as well

as decrease the size of the pores, and consequently, decrease the rock capacity to store fluids. Figure 10 represents a color map to illustrate the distribution of the highest concentration elements that were identified in the X-ray Fluorescence method, summarized in Table 1.

Figure 8: *Image of tar sandstone obtained by SEM, with some highlighted pores*.

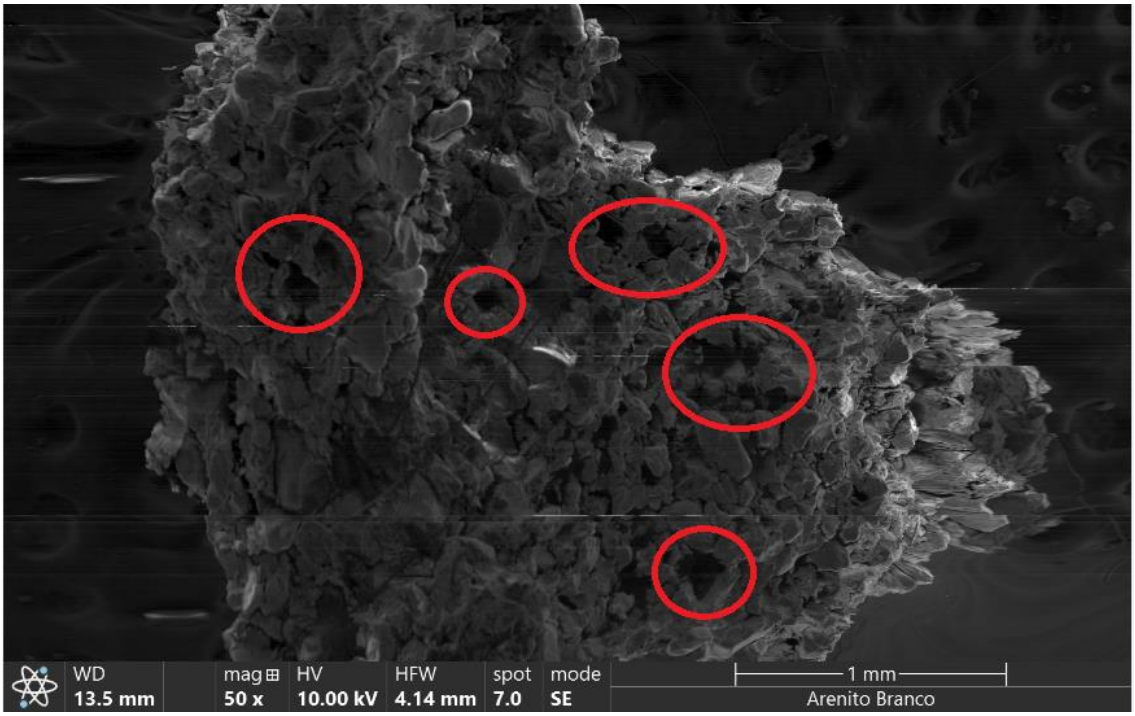

Figure 9: *Cement free particles, giving good reservoir quality to tar sandstone.*

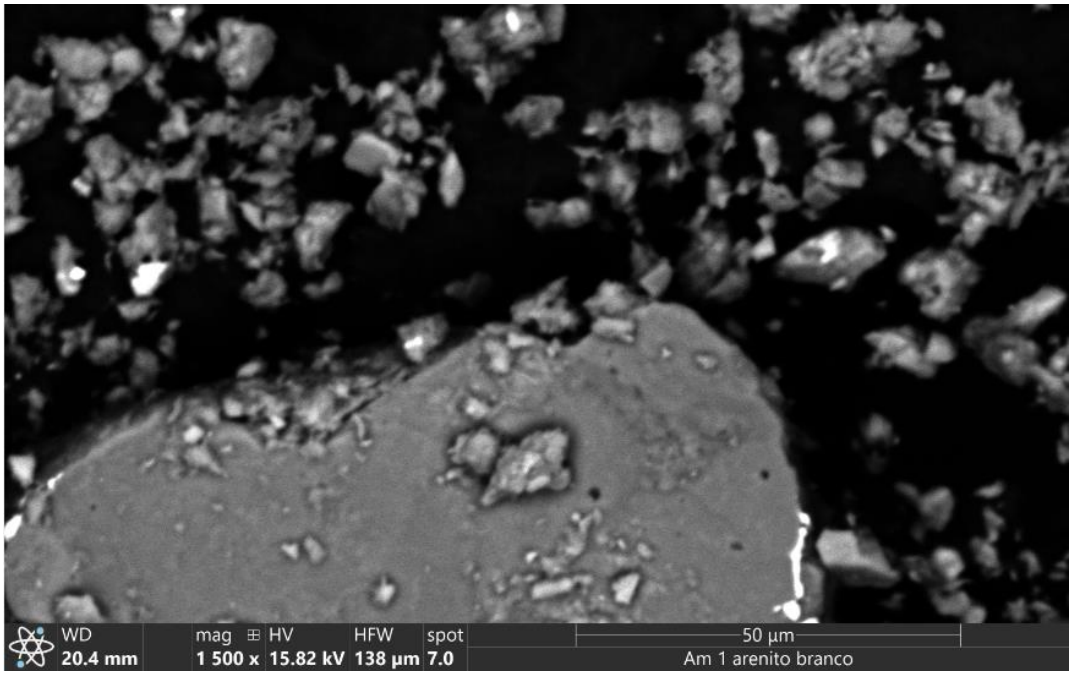

Figure 10: *Proportion of the highest concentration elements identified in XRF and illustrated in SEM.*

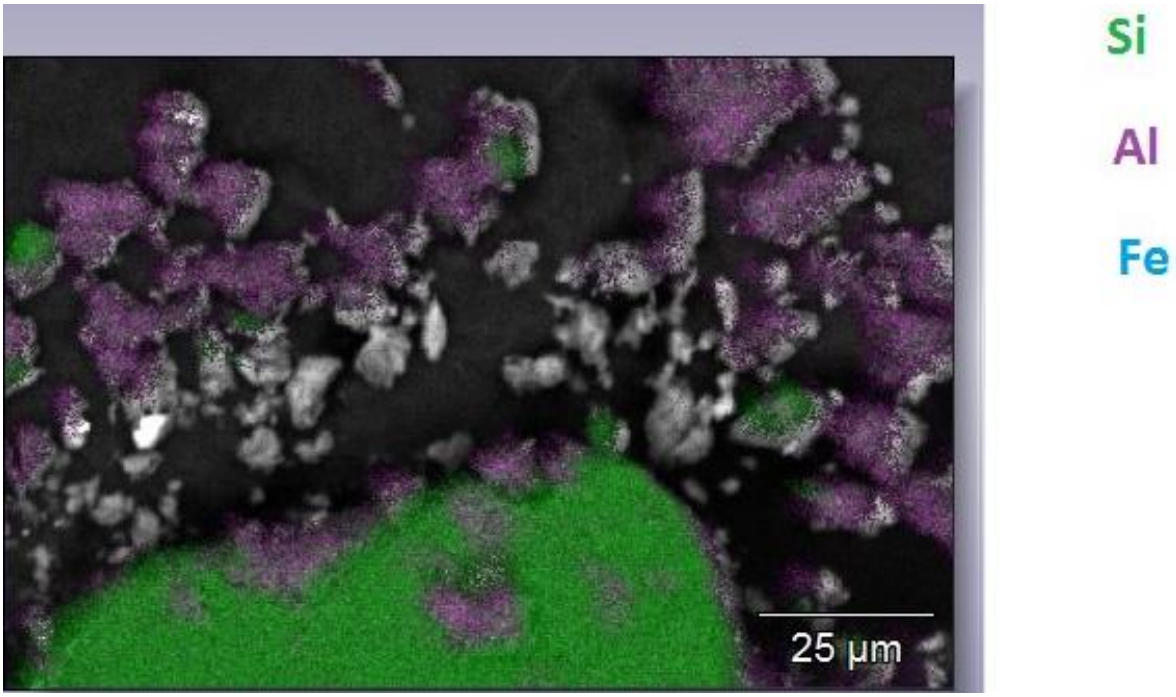

Figure 11 is the reconstructed image of a slice of the tar sandstone internal structure, by gamma - ray computed tomography (tar sandstone from Paraná Basin). It is worth remembering that this was a non-destructive method, i.e., the sample was placed on the tomograph in the same way as it was collected from the outcrop, without being sprayed. The image was reconstructed using ML-ME Software algorithm and implemented in the MATLAB platform.

From the image obtained, it is possible to see, clearly, the voids contained in the tar sandstone matrix and their connections, which are represented by the dark blue color, in Figure 11. The purple color represents the heaviest material comprising the rock, that is, its solid part.

Figure 11: *Reconstructed image of the internal structure of a sample slice, obtained by the third generation computerized industrial tomograph.*

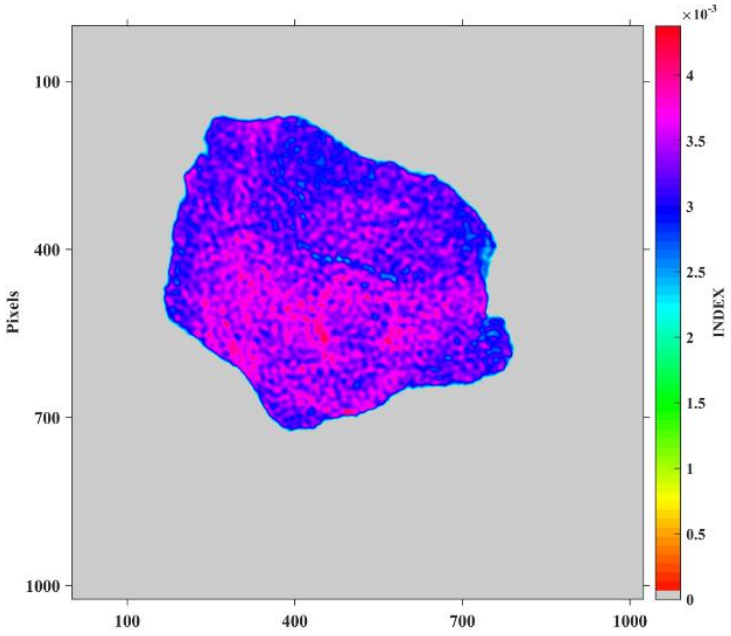

4. CONCLUSION

The tar sandstone analyzed by the X-ray fluorescence technique was, predominantly, composed of Si (23.9%), Al (7.44%) and K (1.44%). Several elements in lower concentration were, also, found (in the order of ppm).

From X-ray Diffraction, it was possible to identify the peaks of the main crystalline phases present in the sample, namely Quartz, Microcline and Hydrobiotite. These crystalline phases have, in their chemical composition, the elements that were identified in the highest concentration by X-ray fluorescence, what means, in this case, that one technique complemented the results of the other.

The scanning electron microscope allowed images of the grain morphology to be obtained in large amplitudes, as well as the visualization of the sample empty spaces (pores) that store the oil. It was verified that there is no cementation between the grains, what gives the tar sandstone the characteristics of a good reservoir.

From the image reconstructed by the third generation computerized industrial tomograph, it was possible to observe the pores of the rock matrix, as well as the way the pores are connected, giving the tar sandstone two typical characteristics of an excellent hydrocarbon reservoir: high porosity and high permeability.

ACKNOWLEDGMENT

The authors express their acknowledgment to CNEN, CNPq and IAEA for the financial support and IGC/USP for the collection of the tar sandstone rock and preparation of the sample. Thiago L. S. Bernardes thanks CAPES, Rafael A. Amadeu thanks CNEN and Rodrigo S. Santos and Alexandre F. Velo thank CNPq for their fellowship. Margarida M. Hamada and Carlos H. de Mesquita thank CNPq for their research productivity scholarship.

REFERENCES

[1] SUGUIO, Kenitiro. Tipos de Rochas Sedimentares. In: SUGUIO, Kenitiro. **Rochas Sedimentares.** São Paulo: Edgard Blucher Ltda, 1980. p. 138- 139.

[2] ARAÚJO, C. C., YAMAMOTO, J.K., MADRUCCI, v. **Análise Morfoestrutural em área de ocorrência de arenito asfáltico, Bacia do Paraná, São Paulo.** Instituto Geológico, São Paulo, v. 24, n. 1-2, p.25-41, ago. 2003.

[3] FILHO, A. T., 1982, **"Ocorrência de arenito betuminoso em Anhembi (SP) - cubagem e condicionamento geológico".** Anais do XXXII Congresso Brasileiro de Geologia Salvador / Bahia , v.l 5 , pp: 2344 - 2348.

[4] CABRAL, C. V.. **Análise de biomarcadores nos arenitos asfálticos da borda leste da Bacia do Paraná.** 2006. 211 f. Dissertação (Mestrado) - Curso de Engenharia Civil, Universidade Federal do Rio de Janeiro, Rio de Janeiro, 2006.

[5] OSERN, 2003 **"Oil Sands Reclamation Research Network"**, Universidade de Alberta, http:\\www.rr.ualberta.ca/oilsainds.

[6] GREG M. BANIAK, MURRAY K. GINGRAS, BEVERLY A. BURNS, S. GEORGE PEMBERTON. **PETROPHYSICAL CHARACTERIZATION OF BIOTURBATED SANDSTONE RESERVOIR FACIES IN THE UPPER JURASSIC ULA FORMATION, NORWEGIAN NORTH SEA, EUROPE**. Journal of Sedimentary Research 85: 62-81,2015.

[7] CNUDDE V. M., J. BOONE, DIERICK M., VAN HOOREBEKE L. , JACOBS P. **3D characterization of sandstone by means of X-ray computed tomography.** Geosphere 7 (1): 54-61, 2011.

[8] CHARALAMPIDOU, E-M., HALL, S. A., STANCHITS, S., VIGGIANI, G., LEWIS H. - **Characterization of Shear and Compaction Bands in Sandstone Using X-Ray Tomography and 3D Digital Image Correlation. In: Advances in Computed Tomography for Geomaterials: GeoX 2010.** Edited by Khalid A. Alshibli and Allen H. Reed. Chapter 7, 2013.

[9] JARZYNA, J.A., KRAKOWSKA,P.I., PUSKARCZYK, E., WAWRZYNIAK-GUZ, K., BIELECKI, J., TKOCZ,K., TARASIUK, J., WROŃSKI, S., DOHNALIK, M. **X-ray computed microtomography—a useful tool for petrophysical properties determination. Computational Geosciences,** 20(5): 1155–1167, 2016.

[10] DE MESQUITA, C.H. ; VELO, A.F. ; CARVALHO, D.V.S. ; MARTINS, J.F.T. ; HAMADA, M.M. **Industrial tomography using three different gamma ray. Flow Measurement and Instrumentation,** v. 47, p. 1-9, 2016.

[11] DE MESQUITA, CARLOS HENRIQUE ; DE SOUSA CARVALHO, DIEGO VERGAÇAS ; KIRITA, RODRIGO ; VASQUEZ, PABLO ANTONIO S. ; HAMADA, MARGARIDA MIZUE **. Gas-liquid distribution in a bubble column using industrial gamma-ray computed tomography. Radiation Physics and Chemistry** v. 95, p. 396-400, 2014.

[12] MESQUITA, C. H. ; CALVO, W. A. P. ; CARVALHO, D. V. S. ; Sprenger, E.Ss ; KIRITA, R. ; VASQUEZ, P. A. S. ; COSTA, F. E. ; Hamada, Margarida M. . **Development of the Mechanical System on a Development of the Mechanical System on a Scanner in Brazil. Journal of Physical Science and Application,** v. 2, p. 158, 2012.

[13] **"Fundamentos teóricos da técnica de análise espectrométrica por fluorescência de raios-x"**, https://www.maxwell.vrac.puc-rio.br/18799/18799_6.PDF (2011).

[14] **"Difração de Raios X"**, http://www.angelfire.com/crazy3/qfl2308/1_multipart_xF8FF_2_DIFRACAO.pdf (2013).

[15] DEDAVID, Berenice Anina; GOMES, Carmen Isse; MACHADO, Giovanna. "**Microscopia Eletrônica de Varredura: Aplicações e Preparação de Amostras"**. Porto Alegre: Edipucrs, 2007.

[16] IAEA-TECDOC-1589 Industrial Process Gamma Tomography, Viena, Maio 2008.